RSC Advances

PAPER

View Article Online
View Journal | View Issue

Cite this: *RSC Adv.*, 2025, **15**, 8411

A facile smartphone-based digital image colorimetric sensor for the determination of tetracyclines in water using natural phenolic compounds induced to grow gold nanoparticles†

Kraingkrai Ponhong, [a] Tammanoon Nilnit, [a] Chang Young Lee, [b] Worapan Kusakunniran, [c] Phoonthawee Saetear[de] and Sam-ang Supharoek *[fg]

Received 5th January 2025
Accepted 10th March 2025

DOI: 10.1039/d5ra00091b

rsc.li/rsc-advances

A cost-effective smartphone-based digital image colorimetric sensor was developed to determine tetracyclines by inducing *in situ* growth of gold nanoparticles using naturally occurring phenolic compounds derived from para rubber tree bark waste. The green intensity of the purple-red product was measured using smartphone-based digital image analysis. Under optimal conditions, the calibration graph exhibited linearity within the range 0.05 to 0.50 μg mL^{-1}, with a coefficient of determination (R^2) of 0.9940. The limits of detection (LOD) and limits of quantitation (LOQ) were 15 and 50 ng mL^{-1}, respectively, with levels of precision for intraday and interday less than 3.91% and 4.59%, respectively. The proposed method was effectively validated to determine the spiked tetracycline antibiotics in water samples, achieving a high relative recovery rate ranging from 86.4% to 114.4%. Our method is facile, convenient, dependable, and verifiable as an alternate procedure for measuring tetracycline levels in water.

Introduction

Tetracycline antibiotics (TCs) are commonly used to treat bacterial infections in veterinary and animal husbandry because of their low price and good antibacterial activity against both Gram-positive (+) and Gram-negative (−) bacteria.[1–5] However, tetracyclines do not degrade easily in animals, and large amounts of undegraded antibiotics are excreted and introduced into the environment, contaminating soil and water ecosystems. Tetracyclines have low biodegradability and accumulate in the human body *via* the food chain, impacting human health even at low dosages[6] through abdominal discomfort, epigastric pain, nausea, vomiting, and anorexia.[7] Environmental pollution caused by antibiotic residues in water is now a worldwide concern.[8,9] The maximum residue limits (MRLs) of antibiotic residues in water have not been established due to a lack of data.[10] Thus, a simple, inexpensive, rapid, and sensitive analytical method for detecting and monitoring environmental pollution caused by antibiotic residues is required.

Several analytical techniques have been used to determine tetracyclines such as capillary electrophoresis,[11] electrochemical,[12] surface enhanced Raman spectroscopy (SERS),[13] fluorescence,[14] LC-MS,[15] and HPLC.[1,3,6,16] These approaches have high precision and outstanding specificity but drawbacks include time-intensive procedures, substantial waste production, the need for costly equipment, and the requirement for highly proficient professionals, making them inappropriate for simple, fast, on-site detection. An alternative procedure based on colorimetry is facile, convenient, and sensitive. Several types of tetracycline sensors have been developed including quantum dots,[17–19] gold and silver nanoclusters,[20,21] colorimetric sensors,[22] gold nanoclusters,[21,23–25] and gold nanoparticles (AuNPs).[5,26–35]

Nowadays, AuNPs are extensively utilized in analytical chemistry owing to their distinctive physical and chemical characteristics.[36] The surface plasmon resonance (SPR) of AuNPs is influenced by the size, shape, and aggregation state of the particles, while the intensity of the absorbance band is

[a]*Multidisciplinary Research Unit of Pure and Applied Chemistry, Department of Chemistry, Center of Excellence for Innovation in Chemistry, Faculty of Science, Mahasarakham University, Maha Sarakham 44150, Thailand*

[b]*School of Energy and Chemical Engineering, Ulsan National Institute of Science and Technology (UNIST), Ulsan 44919, Republic of Korea*

[c]*Faculty of Information and Communication Technology, Mahidol University, 999 Phuttamonthon 4 Road, Salaya, Nakhon Pathom 73170, Thailand*

[d]*Department of Chemistry, Faculty of Science, Mahidol University, 272 Rama VI Road, Ratchathewi, Bangkok 10400, Thailand*

[e]*Flow-Innovation Research for Science and Technology Laboratories (FIRST Labs), Department of Chemistry, Center of Excellence for Innovation in Chemistry, Faculty of Science, Mahidol University, 272 Rama VI Road, Ratchatawi, Bangkok 10400, Thailand*

[f]*Department of Medical Science, Mahidol University, Amnatcharoen Campus, Amnat Charoen 37000, Thailand. E-mail: samang.sup@mahidol.ac.th*

[g]*Department of Chemistry, Center of Excellence for Innovation in Chemistry, Faculty of Science, Mahidol University, Bangkok 10400, Thailand*

† Electronic supplementary information (ESI) available. See DOI: https://doi.org/10.1039/d5ra00091b

directly proportional to the concentration of AuNPs in solutions. Therefore, AuNPs capped with various reagents possess unique advantages in colorimetric analysis, yielding a visible color change in the solution. Synthetic, toxic, and expensive capping agents including aptamers,[5,32,33,35] cetyltrimethylammonium chloride,[27] methylene blue,[28] $MnFe_2O_4$-Au (MFO-Au),[29] and cysteamine[34] have been reported for tetracycline determination.

Cost-effective smartphone-based digital image approaches have successfully applied intelligent strategies to evaluate the colorimetric method, allowing for rapid and accurate quantitative analyses of various interested analytes such as pesticide residue,[37] toxic metal,[38] protein,[39] pharmaceutical,[40] phenolic,[41] uric acid,[42] and tetracyclines.[43–45] Green analytical chemistry focuses on choosing and creating effective evaluation techniques that produce minimal waste and utilize natural substances that are safe for humans and the environment. Natural reagents are the preferred option for choosing and implementing environmentally friendly methods. Numerous sources of reagents including natural phenolics, natural peroxidase enzymes, and tannins have been documented as alternatives to harmful and costly synthetic compounds for the determination of ferric ion, carbaryl, and nitrite.[3,46–49]

This study developed a smartphone-based digital image colorimetric sensor to quantify tetracycline contamination in water samples. The sensor was based on the *in situ* growth of gold nanoparticles induced by an unrefined solution of natural phenolic compounds derived from waste para rubber tree bark (*Hevea brasiliensis* Muell. Arg.). Natural phenolic-rich hydroxyl groups serve as effective reducing and stabilizing agents for gold chloride in the presence of tetracyclines, leading to the growth of AuNPs. The efficiency of our developed approach for colorimetric sensors was evaluated and optimized by examining various parameters.

Results and discussion

Preliminary reaction for the determination of tetracyclines using AuNP production induced by natural phenolic compounds

The proposed reaction to analyze tetracycline levels was examined by mixing a solution of gold chloride and a natural phenolic compound derived from rubber tree bark in the presence of tetracyclines under alkaline conditions. The solution mixture facilitated the synthesis of AuNPs, resulting in a purple-red product. The surface plasmon resonance (SPR) of the AuNPs was detected at a wavelength of 540 nm utilizing a UV-visible absorption spectrophotometer (Fig. 1A).

Different conditions were also examined, as shown in Fig. S1.† Under alkaline conditions (pH > 7), we observed the purple-red color of the AuNPs in combination with additional natural phenolic compounds (Fig. S1A†). Adding tetracycline increased the color intensity (Fig. S1B†). The SPR presented in Fig. 1A indicated that partial synthesis of the AuNPs was finalized with the incorporation of tetracycline.

The addition of tetracycline increased the absorbance at a constant wavelength, indicating higher AuNP concentration

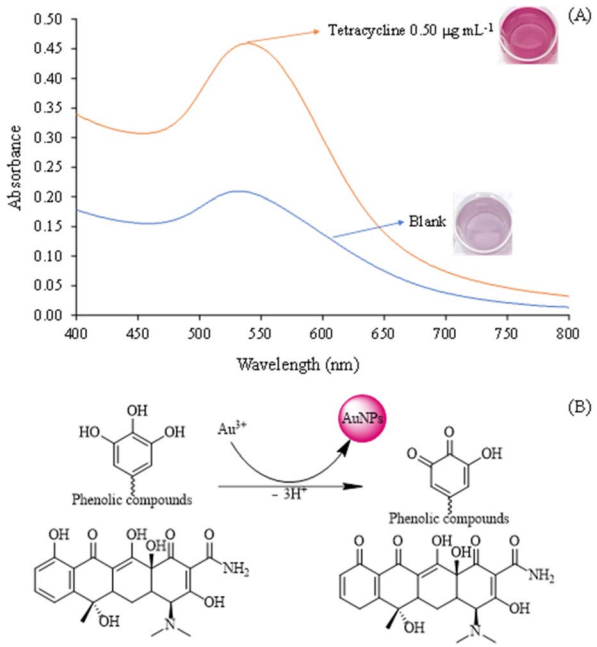

Fig. 1 Gold nanoparticle formation induced by natural phenolic compounds, (A) surface plasmon resonance (SPR) of gold nanoparticles and (B) a possible reaction path.

rather than aggregation. The colors displayed in Fig. S1A–C† further corroborated this assertion. Phenolics, naturally sourced from rubber tree bark waste, function as reducing and stabilizing agents for stimulating the growth of AuNP synthesis,[50] while tetracycline can completely reduce aurate salts to form AuNPs.[27] One possible reaction is presented in Fig. 1B. Phenolic compounds directly reduce Au^{3+} to AuNPs without the need for a catalyst or seed nanoparticles, while Au^{3+} converts phenolic groups into their respective quinones by transferring H^+, resulting in AuNP formation.[27,51]

The specificity and selectivity of the colorimetric sensor was examined using three widely used antibiotics, namely oxytetracycline (OTC), chlortetracycline (CTC), and doxycycline (DC) which are structurally identical compounds. The results indicated that these three antibiotics facilitated the growth of AuNPs in a manner analogous to tetracyclines. Another sulfonamide antibiotic yielded a distinct SPR due to its aggregation with AuNPs under particular conditions, as depicted in Fig. S2.† The AuNP colorimetric sensor achieved selective detection of tetracyclines.

Transmission electron microscopy (TEM) and dynamic light scattering measurements were conducted using a Zetasizer to clarify the morphological characteristics and size distribution alterations of AuNPs synthesized under optimal conditions. The AuNPs (blank) consistently exhibited a range of sizes (Fig. 2A and C), demonstrating a high degree of separation without the adhesion of spherical particles. The AuNP particle diameters were 5 to 13 nm (mean 10.78 ± 2.73 nm). The addition of tetracycline resulted in a higher concentration of AuNPs with an average diameter of 11.21 ± 3.77 nm (Fig. 2B and D). There was no significant difference between the average size distribution

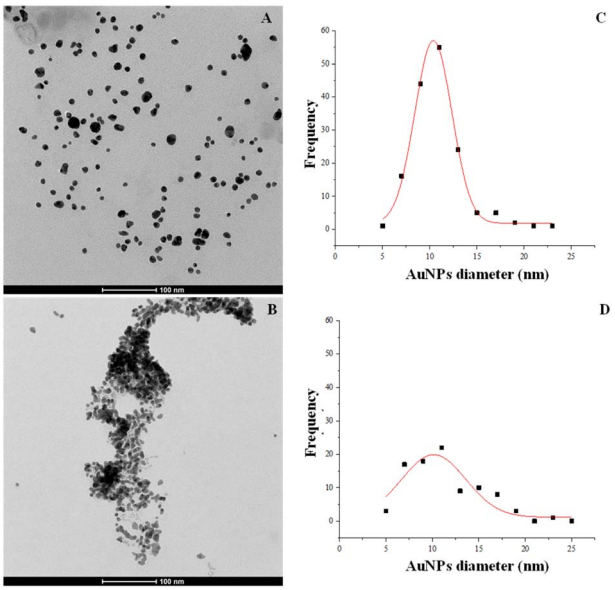

Fig. 2 The morphology and diameter of AuNPs, TEM image of AuNPs (A) without TC, (B) with TC, AuNP size distribution (C) without TC, and (D) with TC.

of AuNP stimulated growth using natural phenolic compounds with and without tetracyclines evaluated by one-way ANOVA ($p > 0.05$). Therefore, the AuNPs remained unaggregated following the addition of tetracycline.

To confirm the presence of phenolic compounds, especially tannic acid, the functional groups of the natural reagent extract utilized to synthesize AuNPs were analyzed using FTIR and compared to standard tannic acid. The IR spectra of the natural reagent extract were superimposed with standard tannic acid, as depicted in Fig. S3.† The natural reagent displayed distinctive peaks corresponding to numerous functional groups including O–H stretching (3243 cm^{-1}), C–H stretching (2930 cm^{-1}), C=O stretching (1716–1594 cm^{-1}), aromatic C=C stretching (1594 cm^{-1}), and carboxyl C–O stretching at 1385 cm^{-1}. The C–C stretching, C–O stretching, and O–H bending peaks were identified between 1594 and 1033 cm^{-1}. The functional groups of the natural reagent extract corresponded to those of standard tannic acid (Fig. S3†). Furthermore, to validate the potential reaction among $AuCl_3$, TC, and natural phenolics, FTIR analysis was conducted, and the results are illustrated in Fig. S3.† The FTIR spectra indicated an enhancement in the stretching vibration of C=O within the range of 1643 to 1597 cm^{-1} in quinone. A peak of phenolic O–H bending at 1385–1272 cm^{-1} was deformed, signifying that the phenolic hydroxyl groups facilitated the spontaneous reduction of Au^{3+} through phenol-to-quinone oxidation.[52]

The SPR of AuNPs caused by a natural phenolic compound, specifically tannic acid, in the presence of tetracycline was assessed, with the findings presented in Fig. S4.† The AuNPs synthesized using natural reagents exhibited a characteristic SPR spectrum that was identical to tannic acid. Natural reagents contain phenolic compounds such as tannic acid, serving as both reducing and stabilizing agents to synthesize AuNPs.[50,53]

Optimization of parameters for tetracycline determination by smartphone-based digital images under a light control box.

A built-in white full LED interior illumination was located on the top of a light control box cabinet. This obviated the necessity of using flash photography to obtain photos and regulated light intensity consistency (Fig. S5†). The images obtained from the 96-microwell plate were analyzed to evaluate the consistency of light irradiation from the LEDs by measuring the repeatability of RGB intensities. At a tetracycline concentration of 0.30 μg mL^{-1}, the RSD was less than 4.40% ($n = 96$), demonstrating a high level of repeatability in measuring the intensity of green light under the control condition of the light control box. The slope of the RSD obtained from the calibration graph, established using the tetracycline standard in the concentration range 0.05 to 0.50 μg mL^{-1}, was less than 4.90% ($n = 5$). Our results revealed that the light within the closed light control box had no significant impact on green intensity.

The AuNP color product was transferred to a 96-microwell plate and captured as a digital image using a smartphone under controlled lighting conditions in a light control box. The RGB intensity of the acquired image was assessed using ImageJ software to obtain the RGB profile, as illustrated in Fig. 3A. To determine the concentration of tetracycline, a graph was created to show the difference in RGB intensity (ΔI) between the reagent blank zone and the standard, plotted against tetracycline concentrations of 0.0 to 0.50 μg mL^{-1} (Fig. 3B). The intensities of the green (G), blue (B), and red (R) channels in the acquired image were directly related to the concentration of tetracycline,

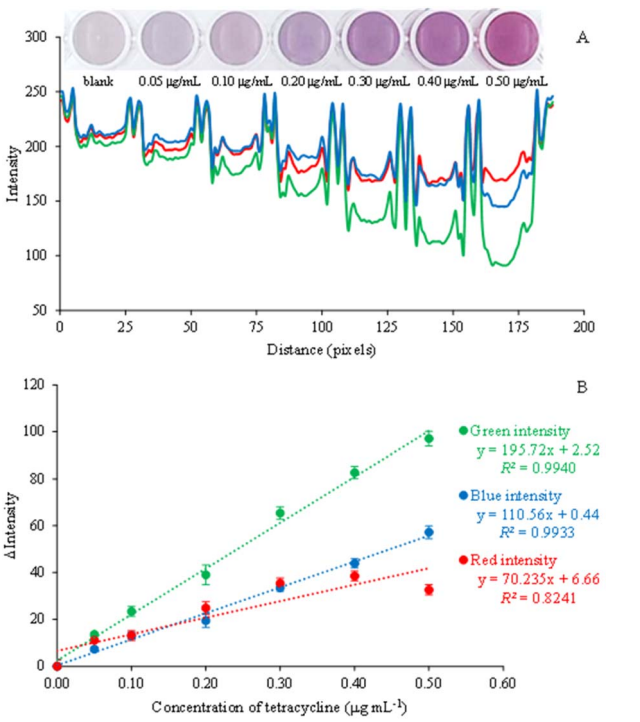

Fig. 3 RGB profiles of purple-red gold nanoparticles (A), and a calibration graph from 0.00 to 0.50 μg mL^{-1} of tetracycline at different RGB intensities (B).

with the green intensity exhibiting the highest level of sensitivity. Thus, the proposed method was used to determine the concentration of tetracycline by measuring the intensity of the green color. The sensitivity of the procedure was determined by varying the volume of the product solution in the microwell plate. The volumes tested were 50, 100, 150, 200, 250, and 300 μL. The sensitivity increased 4.65-fold from 50 to 300 μL loading volume (Fig. 4A). A maximum volume of 300 μL was placed into the 96-microwell plate for the determination of tetracycline.

Optimized conditions for the determination of tetracycline using AuNP stimulation with phenolic natural extract

Effect of gold chloride concentration. Gold chloride is a crucial component in the production of AuNPs through its reaction with natural phenolic compounds and tetracycline under basic conditions. The gold chloride concentration was investigated at 0.5, 1.0, 2.0, and 3.0 mmol L^{-1}, with results indicating a considerable rise in the slope of the calibration graph, ranging from 0.5 to 3.0 mmol L^{-1}. A concentration of 1.0 mmol L^{-1} gold chloride was chosen for the subsequent experiment due to the sufficient sensitivity demonstrated in Fig. 4B for the proposed method.

Effect of natural phenolic extract volume. The volume of natural phenolics was researched at 20, 40, 60, 80, and 100 μL. The intensity increased from 20 to 60 μL and then decreased above 60 μL, as depicted in Fig. 4C. Therefore, a natural phenolic extract volume of 60 μL was chosen for subsequent experiments to induce the formation of AuNPs. The natural reagents extracted from rubber tree bark contain natural phenolics such as tannic acid[54] which acts as a metal-chelating agent because it contains numerous hydroxy groups and also serves as a reducing reagent[50]

Effect of NaOH concentration. In the preliminary investigation, the reaction between gold chloride, natural phenolics, and tetracycline resulted in the formation of AuNPs as purple-red products under alkaline conditions. The concentrations of NaOH at 0, 1, 3, 5, and 7 mmol L^{-1} were examined. The signal increased gradually from 0 to 1 mmol L^{-1}, followed by a sharp decline after reaching 1 mmol L^{-1}, as shown in Fig. 4D. High

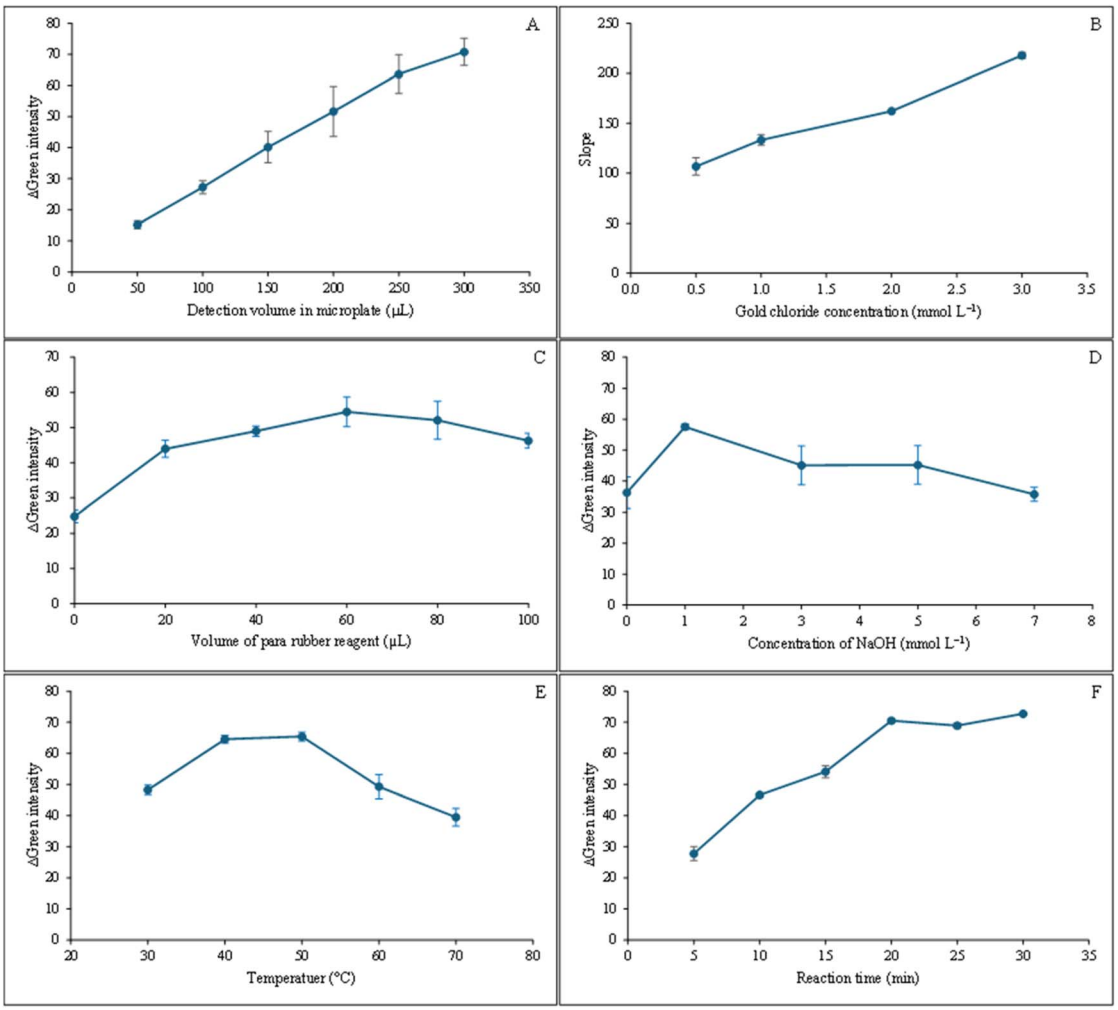

Fig. 4 Optimal conditions for the determination of tetracycline using AuNPs induced by natural phenolic compounds, (A) detection volume in microplate, (B) effect of gold chloride concentration, (C) effect of para rubber reagent volume, (D) concentration of NaOH, (E) effect of temperature, and (F) effect of reaction time.

concentrations of NaOH generated excessive hydroxide anions (OH^-) that reacted with $AuCl_3$, resulting in the formation of $Au(OH)_3$ precipitates instead of AuNPs. Therefore, a concentration of 1 mmol L^{-1} of NaOH was used for the next procedure.

Effect of incubation temperature and incubation time. Incubation temperatures ranging from 30 to 70 °C were investigated. The sensitivity of the proposed approach for determining tetracycline increased from 30 to 40 °C. The signals leveled off over 40 to 50 °C. After reaching 50 °C, the sensitivity dropped (as shown in Fig. 4E). The stability of the analyte diminished at elevated temperatures. Therefore, a temperature of 40 °C was selected as optimal for AuNP growth.

Employing longer incubation periods resulted in enhanced production of AuNP products generated by the proposed reaction. Incubation times ranging from 5 to 30 min were examined. The sensitivity showed a notable increase from 5 min to 20 min. When reaching 20 min, the signal stabilized and exhibited no further alterations (Fig. 4F). Therefore, a 20 min incubation time was selected for the next procedure since it provided adequate sensitivity for determination and a short analysis time.

Analytical characteristics. Under the optimal experimental conditions (Table S1†), the smartphone-based digital images of the AuNP colorimetric sensor showed a linear correlation with concentrations of tetracycline ranging from 0.05 to 0.50 μg mL^{-1}. The linearity was confirmed by a good coefficient of determination (R^2) value of more than 0.99 (Fig. 3B). The limit of detection (LOD) and limit of quantitation (LOQ) were determined using the formulas 3 SD/slope and 10 SD/slope, respectively where SD represents the standard deviation of the blank. The LOD and LOQ were 15 and 50 ng mL^{-1}, respectively. The smartphone-based digital image sensor exhibited a precision of 3.91% when analyzing tetracycline intraday at a concentration of 0.30 μg mL^{-1} ($n = 7$). Using different batches of natural phenolic compound extracts to synthesize AuNPs in the presence of tetracycline resulted in colorimetric sensor repeatability of 4.59% over 7 days ($n = 3 \times 7$). Natural reagent extracts from different batches generated AuNPs. To mitigate the experiment's inherent unpredictability while utilizing natural phenolic extracts, we generated the calibration graph daily.

Interferences for the determination of tetracyclines. The optimized approach was used to investigate interferences in water samples by adding a 0.30 μg mL^{-1} tetracycline standard solution with different amounts of foreign ions. Tolerance limits of various interferences for tetracycline investigation were determined as SO_4^{2-}, CO_3^{2-} (15 μg mL^{-1}), NO_2^-, NO_3^-, Cl^- (10 μg mL^{-1}), CH_3COO^-, Hg^{2+}, Pb^{2+}, Cr(VI), PO_4^{3-}, 1-naphthol (1.0 μg mL^{-1}), Mn^{2+}, Ni^{2+}, Ca^{2+}, In^{3+} (0.5 μg mL^{-1}), Zn^{2+}, Mg^{2+}, Sc^{2+}, Cd^{2+} (0.3 μg mL^{-1}), and Cu^{2+}, Fe^{3+} (0.1 μg mL^{-1}). Results indicated that most ions interfered with tetracycline determination at low concentrations. Thus, tetracycline residues in water samples should be extracted using ACN with sugaring-out extraction[55,56] as described in the sample preparation before quantification by the proposed method.

Application to determine tetracyclines in water samples. Tetracycline residues in water samples were extracted using ACN to mitigate potential interference from other ions in the measurement process. The matrix effect (% ME) of spiking ACN at 0.50 mL was determined as 88.9% and this diminished to 61.9% when utilizing ACN at 1.0 mL. The % ME was assessed by contrasting the slope of the calibration graph with and without the matrix. The % ME approached 100%, signifying that matrix negligibility influenced the assessment of the target analyte.[1] The calibration curve for the determination of tetracycline was created by adding 0.50 mL of ACN to the standard tetracycline at a concentration range of 0.05 to 0.50 μg mL^{-1}. The smartphone-based digital images of the AuNP colorimetric sensor were applied to determine tetracycline residues in six water samples, with results presented in Table 1. Tetracycline was not detected in any of the water samples. Recoveries investigated by spiking the tetracycline standard at 0.05 and 0.10 μg mL^{-1} in the water samples ranged from 86.4 to 114.4%, while recoveries obtained from the HPLC-UV reference method ranged between 82.0 and 117.3%. Recoveries obtained from the developed approach did not significantly differ from the HPLC-UV standard method at a 95% confidence level (t stat = 0.368, t critical = 2.220), indicating that our method was accurate and reliable for the determination of tetracycline.

Table 2 summarizes the analytical characteristics of our proposed method compared to several spectrophotometric

Table 1 Recovery of the proposed method for the determination of tetracycline in water samples ($n = 3$)

		TC content by the purposed method			TC content by the standard HPLC-UV		
	Spiked TC (μg mL^{-1})	Found (μg mL^{-1})	Recovery (%)	% RSD	Found (μg mL^{-1})	Recovery (%)	% RSD
1	0.05	0.043	86.4	7.2	0.045	90.4	0.4
	0.10	0.114	114.4	8.7	0.117	117.3	0.0
2	0.05	0.049	98.0	1.2	0.045	90.0	4.3
	0.10	0.101	101.0	9.4	0.110	109.6	3.9
3	0.05	0.046	92.4	3.7	0.044	88.1	2.5
	0.10	0.104	104.0	4.0	0.110	110.4	2.7
4	0.05	0.055	110.3	3.4	0.043	86.0	6.4
	0.10	0.100	100.0	5.9	0.098	98.0	6.2
5	0.05	0.044	87.7	4.8	0.043	86.6	6.1
	0.10	0.088	87.5	1.8	0.098	98.0	3.0
6	0.05	0.045	90.7	2.2	0.041	82.0	1.0
	0.10	0.096	96.3	1.5	0.100	100.0	6.8

Table 2 Comparison of the proposed method and previously reported research for the determination of tetracycline in real samples using AuNPs

Stabilizing/capping agent	Sample	Analyte	Detection	Incubation temp. (°C)	Linear range (μg mL^{-1})	LOD (μg mL^{-1})	Recovery	RSD	Ref.
Aptamer	Drinking water milk, meat	TC	Naked eye	100	2.22×10^{-8} to 2.22	2.22×10^{-9}	86–112%	<5%	5
β-Agonists	Urine	TC	Spectrophotometer	70	5 and 150	0.020–0.50	—	—	27
Aptamer	Honey	TC	Spectrophotometer	Room temp.	0.00001–0.010	0.0000027	91.50–95.33%	<5%	35
Aptamer	Water	TC	Spectrophotometer	Room temp.	0.04 to 2.22	0.031	106.7–115.6%	—	32
ssDNA aptamer	—	OTC	Spectrophotometer	Room temp.	0 to 0.033	0.011	—	—	33
Cysteamine-stabilized	Raw milk	TC	Spectrophotometer	20	0.20–2.0	0.039	91.28–100.87%	<3.09%	34
Natural phenolic compounds	Water	TC	Smartphone-based digital image	40	0.05–0.50	0.015	86.4–114.4%	<5%	This method

methods and digital image colorimetry. Our developed approach provided an alternate facile, sensitive, and environmentally friendly method for detecting tetracycline. The proposed procedure downscaled the volume operation into a microliter, resulting in reduced waste generation. Exploiting a smartphone as an acquisition tool provided rapidity and traceability for tetracycline detection.

Assessing the greenness of the smartphone-based digital image AuNP colorimetric sensor. The Analytical Eco-Scale and Analytical GREEnness Metric Approach were utilized to assess the environmental impact of smartphone-based digital image AuNP colorimetric sensors for tetracycline detection. Table S2 and Fig. S6† display the analytical Eco-Scale score results and the overall AGREE analysis, respectively. The developed approach had high efficacy for green analysis, as evidenced by an analytical Eco-Scale score of 82. An AGREE method evaluation showed that our proposed method yielded a final score of 0.51 and displayed the appearance of yellow. The analytical Eco-Scale assigns penalty points (PPs) to the characteristics of an analytical process. Values above 75 indicated high green analysis, ratings ranging from 50 to 75 signify satisfactory green analysis, and scores below 50 denote insufficient green analysis.[57] The AGREE protocol corresponds to the 12 fundamental principles of green analytical chemistry (GAC). The score achieved was nearly 1 on the green color scale, signifying that the approach represented an exemplary green analysis.[58] Our smartphone-based digital image colorimetric sensor utilizing AuNPs for the quantification of tetracycline fell within the area of green analytical chemistry.

Experimental

Materials and methods

All reagents used in this research were of analytical grade. The tetracycline hydrochloride (TC) standard and gold chloride ($AuCl_3$) were purchased from Sigma-Aldrich (Sigma-Aldrich, Germany). Sodium hydroxide (NaOH) was obtained from (Merck, Germany) Deionized water was sourced from Milli-Q Millipore (Millipore Waters, USA).

A stock solution of tetracycline (1000 mg L^{-1}) was made by dissolving 0.010 g of tetracycline analytical standard in 10.0 mL of methanol. The solution was kept in dark glass bottles at a temperature of 4 °C. The working standard solutions were created daily by gradually diluting the stock solution with deionized water. Stock gold chloride (0.40 mol L^{-1}) was prepared by dissolving 0.50 g of $AuCl_3$ in 4.0 mL of 0.01 mol L^{-1} HNO_3. Sodium hydroxide (1.0 mol L^{-1}) was prepared by weighing 1.00 g of NaOH in 25.0 DI water.

Apparatus

A Shimadzu UV-visible 1900 Spectrophotometer (Shimadzu, Japan) and a 1.00 cm quartz cell were used for the spectrophotometric measurements. The reaction temperature was controlled by a water bath (Julabo, Eco Temp TW12, Germany). A benchtop centrifuge model 1040 series from Labquit (Labquit, England) was employed to eliminate the powder of the rubber tree bark in the extract solutions, yielding a clear supernatant. The rubber tree bark, which served as a natural reagent, was ground using an Electrolux culinary blender model EBR 2601, manufactured by Electrolux in Thailand. An iPhone 11 Pro Max 256 GB, manufactured by Apple in California and assembled in China, was utilized to photograph the color products in a light control box. The ultrawide camera had an aperture of *f*/2.4 and a field of view of 120°. The wide camera had an aperture of *f*/1.8, while the telephoto camera had an aperture of *f*/2.0. The images were analyzed for green intensity using ImageJ software developed by Rasband, W. S. at the U.S. National Institutes of Health.

Light control box

A square metal cabinet light control box model B270 with outer dimensions 49 (w) × 42 (d) × 42 (h) cm (Fig. S5†) was acquired from Sanoto Chaina (Sanoto, China) for photographing the color products. A built-in white full LED interior illumination with a service lifetime exceeding 50 000 h was located on the top of the cabinet. A tray for positioning a 96-microwell plate was affixed to the lower part of the box. A power adapter with an AC voltage range of 100–240 V was activated using an ON/OFF switch. An 80 × 80 mm aperture at the top of the cabinet was

used to record the photographs. The images were captured using the built-in camera of an iPhone 11 Pro Max, manufactured by Apple in Zhengzhou, China. The camera settings were adjusted to vivid mode and a 1.1× manual zoom.

Para rubber tree bark natural reagent preparation and extraction

Para rubber tree (*Hevea brasiliensis* Muell. Arg.) bark was acquired from a locally planted source in Roi-Et Province, Thailand and kept in a thermos flask. The dry latex on the rubber tree bark was removed and the bark was washed with deionized water before chopping into small pieces and drying in an oven at 60 °C for 24 h. The arid bark was pulverized into fine particles using a culinary blender (Electrolux, Thailand), transferred into a polyethylene container, and stored in a desiccator.

A solution of a naturally occurring reagent was created by dissolving 2.0 g of powdered bark in 40 mL of deionized water. The solution was then subjected to an ultrasonic bath heated at 60 °C for 20 min. The obtained solution was subjected to centrifugation at 6000 rpm and then passed through Whatman No. 1 filter paper to separate the reagent powder. The filtered solution was collected in a volumetric flask and diluted with deionized water to a volume of 50.0 mL. The natural phenolic extract solution was stable for 8 h at ambient temperature. The natural reagent was prepared daily to minimize variations in the stability of the extracted solution.

Smartphone-based digital image analysis for the determination of tetracycline

A smartphone-based digital image colorimetric sensor was employed for the determination of tetracycline using natural phenolic extracts from the rubber tree bark to stimulate the growth of AuNPs, as illustrated in Fig. 5. Briefly, 1500 μL of 1.0 mmol L^{-1} $AuCl_3$, 0.50 mL of sample or tetracycline standard, 60 μL of natural phenolic extracted solution, and 50 μL of 1.0 mol L^{-1} NaOH were mixed in a 10.0 mL volumetric flask. The solution was incubated at 40 °C for 20 min, resulting in the appearance of a purple-red color of AuNPs, and then diluted to 10.0 mL using deionized water. A 300 μL aliquot of the resulting solution was transferred to a 96-well microplate and photographed using a smartphone in a controlled lighting box (Fig. S5†). The acquired image was processed using ImageJ to analyze the intensity of the RGB (red, green, and blue) channels. A calibration graph depicted the relationship between the intensity of ΔG and tetracycline concentration in the range 0.05 to 0.50 μg mL^{-1}. The process of analyzing RGB intensity by ImageJ first selected the obtained image. A circular detection area was then established based on the presence of a purple-red hue in the microplate, followed by the process of selecting plugins before the analysis and measurement of RGB values. The fixed-size circular detection zone was relocated to a different place on the microplate holding the analyte, and the process was repeated as described earlier to measure RGB intensity.

Sample preparation

Environmental water samples were collected from Maha Sarakham Province and filtered through a 0.40 μm nylon filter. The tetracycline analyte was extracted from the aqueous phase using ACN with sugaring-out separation.[55,56] A 5.0 mL aliquot of the sample was pipetted and transferred to a centrifuge tube with 5.0 mL of the ACN extraction solvent and glucose at 0.50 g. The solution was agitated vigorously in a vortex for 15 min before centrifuging at 5000 rpm, 10 °C to achieve complete phase separation. The upper phase of the ACN extraction solvent containing tetracycline analyte at 0.50 mL was applied for quantitative analysis.

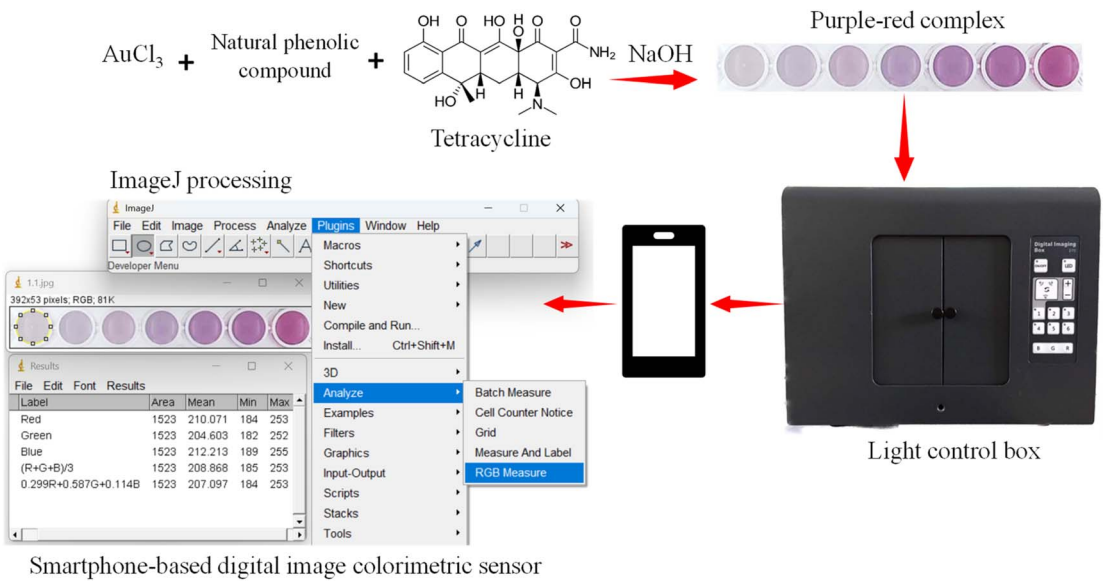

Fig. 5 Smartphone-based digital images for the determination of tetracycline using AuNPs induced by natural phenolic extracts from rubber tree bark.

Interferences investigation

Certain cations and anions affected the analysis of tetracycline using our proposed approach. These interferences could result in inaccurate tetracycline concentrations in actual samples. The interferences, comprising SO_4^{2-}, CO_3^{2-}, NO_2^-, NO_3^-, Cl^-, CH_3COO^-, Hg^{2+}, Pb^{2+}, Cr(VI), PO_4^{3-}, 1-naphthol, Mn^{2+}, Ni^{2+}, Ca^{2+}, In^{3+}, Zn^{2+}, Mg^{2+}, Sc^{2+}, Cd^{2+}, Cu^{2+}, and Fe^{3+}, were examined by augmenting the concentration of the interferent with the analyte of interest at 0.3 μg mL^{-1}. The tolerance limits for each interfering ion were determined as the concentration at which the interference caused a ±10% deviation in intensity relative to the absence of interference.

Morphology and size of AuNPs

AuNPs with and without tetracycline analyte were generated following the method previously outlined. The solution was applied to a copper grid mesh surface 200 (Electron Microscopy Sciences, USA) and the AuNP morphology was examined by TEM. The particle size of the AuNPs was assessed by a Zetasizer (Zetasizer Nano ZS, Malvern Panalytical Ltd., Malvern, England).

HPLC-UV reference method

The HPLC system was used as a standard method[1] for the separation and quantitation of tetracycline residues in water and the results were compared with the developed approach using a Waters 1525 Binary HPLC pump (manufactured by Waters, USA), a Waters 2489 UV-visible detector set at 365 nm, and a Purospher® STAR RP-18 end-capped analytical column (dimensions: 4.6 × 150 mm, particle size: 5.0 μm) (manufactured by Merck, Germany). The specified sample quantity was introduced into the system by injecting 20 μL. Data acquisition was performed using Breeze software version 2.0. The tetracycline was separated by isocratic elution using a mixture of 0.2% trifluoroacetic acid (TFA) in acetonitrile (ACN) and 0.2% TFA at a ratio of 27 : 73 with a flow rate of 0.70 mL min^{-1}.

Conclusions

A facile and reliable method was proposed for *in situ* gold nanoparticle growth induced by natural phenolic compounds derived from the waste of *Hevea brasiliensis* Muell. Arg. bark. A colorimetric sensor using smartphone-based digital images was successfully developed to quantify tetracycline. Natural phenolic compounds that contain hydroxy groups serve as reducing and stabilizing agents for the *in situ* stimulation of AuNP growth. When tetracycline was added, AuNPs were produced, leading to an increase in solution color. A built-in smartphone camera was used to photograph the purple-red-colored product and quantify the tetracycline content. This procedure featuring microliter volume operation was effectively applied to assay the tetracycline residue in water samples. The results showed no significant difference compared to the HPLC-UV reference method at a confidence level of 95%. Our facile, reliable, downscaled, and eco-friendly procedure offers traceability as an alternative method for tetracycline residue quantitation.

Data availability

All data supporting the findings of this study are available from the corresponding author [S.-A Supharoek] on request.

Author contributions

Kraingkrai Ponhong: data curation, formal analysis, funding acquisition, investigation, methodology, resources, validation, visualization, writing – original draft, writing – review & editing. Tammanoon Nilnit: data curation, investigation. Chang Young Lee: writing – review & editing. Worapan Kusakunniran: writing – review & editing. Phoonthawee Saetear: writing – review & editing. Sam-ang Supharoek: conceptualization, data curation, formal analysis, funding acquisition, investigation, methodology, project administration, resources, supervision, validation, visualization, writing – original draft, writing – review & editing.

Conflicts of interest

There are no conflicts of interest to declare.

Acknowledgements

This research project was supported by Mahidol University (Fundamental Fund: fiscal year 2023 (FF-122/2566) and by the National Science Research and Innovation Fund (NSRF), Thailand Science Research and Innovation (TSRI)), and Mahidol University, Amnatcharoen Campus (AM02/2565). K. Ponhong would like to thank Mahasarakham University for financial support (6717004/2567). S. Supharoek would like to thank Mahidol University, Amnatcharoen Campus. K. Ponhong would like to thank the Faculty of Science, Mahasarakham University. The authors express their thanks to the Center of Excellence for Innovation in Chemistry (PERCH-CIC), Ministry of Higher Education, Science, Research and Innovation. Miss Kewalin Nildum, Miss Sirirat Phothiwat, and Miss Patcharapon Jantapitak provided encouragement during the experimental procedures and assisted in creating the figures. The acknowledgements come at the end of an article after the conclusions and before the notes and references.

References

1 N. Nakhonchai, N. Prompila, K. Ponhong, W. Siriangkhawut, J. Vichapong and S.-a. Supharoek, *Talanta*, 2024, **271**, 125645.
2 D. Wu, S. Dai, H. Feng, S. H. P. P. Karunaratne, M. Yang and Y. Zhang, *Environ. Pollut.*, 2024, **341**, 122904.
3 T. Nilnit, J. Jeenno, S.-a. Supharoek, J. Vichapong, W. Siriangkhawut and K. Ponhong, *Food Chem.*, 2024, **437**, 137879.

4 S.-a. Supharoek, K. Ponhong, B. Weerasuk, W. Siriangkhawut and K. Grudpan, *J. Iran. Chem. Soc.*, 2020, **17**, 2385–2395.
5 K. Yang, R. Zhu, Z. Li, S. Shuang, Y. Zhai and C. Dong, *Talanta*, 2024, **266**, 125077.
6 H. Sereshti, F. Karami and N. Nouri, *Microchem. J.*, 2021, **163**, 105914.
7 A. Peng, C. Wang, Z. Zhang, X. Jin, C. Gu and Z. Chen, *Water Res.*, 2022, **225**, 119197.
8 M. A. Shaker, W. H. Alshitari, M. T. Basha, N. A. Aly, M. Asim, H. M. Albishri, S. A. Bhawani and A. A. Yakout, *Mater. Today Commun.*, 2024, **38**, 107869.
9 J. Teng, S. Xiong, F. Li, S. Wang and T. Li, *Appl. Catal. O: Open*, 2024, **191**, 206957.
10 H. Kuang, X. Chen, C. Hao, W. Ma, L. Xu and C. Xu, *RSC Adv.*, 2013, **3**, 17294–17299.
11 L. Nozal, L. Arce, B. M. Simonet, A. Ríos and M. Valcárcel, *Anal. Chim. Acta*, 2004, **517**, 89–94.
12 Y. Meng, Y. Huang, G. Huang and Y. Song, *RSC Adv.*, 2023, **13**, 28148–28157.
13 D. Jin, Y. Bai, H. Chen, S. Liu, N. Chen, J. Huang, S. Huang and Z. Chen, *Anal. Methods*, 2015, **7**, 1307–1312.
14 H. Xie, Y. Lu, R. You, W. Qian and S. Lin, *RSC Adv.*, 2022, **12**, 8160–8171.
15 H.-C. Ri, J. Piao, L. Cai, X. Jin, X. Piao, X. Jin, C.-S. Jon, L. Liu, J. Zhao, H.-B. Shang and D. Li, *Anal. Chim. Acta*, 2021, **1182**, 338957.
16 X. Di, X. Zhao and X. Guo, *J. Sep. Sci.*, 2020, **43**, 3129–3135.
17 W.-J. Wu, Q. Zhao, R. Zhou, Y.-C. Liang, W.-B. Zhao and C.-X. Shan, *Spectrochim. Acta, Part A*, 2021, **259**, 119901.
18 Z. Liu, J. Hou, Q. He, X. Luo, D. Huo and C. Hou, *Anal. Methods*, 2020, **12**, 3513–3522.
19 A. Moaddab and S. Ghasemi, *Microchem. J.*, 2021, **166**, 106222.
20 Y. Zhang, M. Lv, P. Gao, G. Zhang, L. Shi, M. Yuan and S. Shuang, *Sens. Actuators, B*, 2021, **326**, 129009.
21 Y. Song, J. Qiao, W. Liu and L. Qi, *Microchem. J.*, 2020, **157**, 104871.
22 J. Cao, H. Zhang, Q. Nian and Q. Xu, *Int. J. Biol. Macromol.*, 2022, **212**, 527–535.
23 Z. Zhang, Y. Tian, P. Huang and F.-Y. Wu, *Talanta*, 2020, **208**, 120342.
24 X. Yang, S. Zhu, Y. Dou, Y. Zhuo, Y. Luo and Y. Feng, *Talanta*, 2014, **122**, 36–42.
25 Y. Li, Q. Du, X. Zhang and Y. Huang, *Talanta*, 2020, **206**, 120202.
26 Y. Lv, S. Qi, I. M. Khan, X. Dong, M. Qin, L. Yue, Y. Zhang and Z. Wang, *Anal. Chim. Acta*, 2023, **1270**, 341238.
27 L. Shen, J. Chen, N. Li, P. He and Z. Li, *Anal. Chim. Acta*, 2014, **839**, 83–90.
28 Y. Guo, X. Wang and X. Sun, *Int. J. Electrochem. Sci.*, 2015, **10**, 3668–3679.
29 L. Qin, Z. Wang, Y. Fu, C. Lai, X. Liu, B. Li, S. Liu, H. Yi, L. Li, M. Zhang, Z. Li, W. Cao and Q. Niu, *J. Hazard. Mater.*, 2021, **414**, 125448.
30 M. Asadollahi-Baboli and A. Mani-Varnosfaderani, *Measurement*, 2014, **47**, 145–149.
31 N. Naimi-Shamel, P. Pourali and S. Dolatabadi, *J. Mycol. Med.*, 2019, **29**, 7–13.
32 M. Qi, C. Tu, Y. Dai, W. Wang, A. Wang and J. Chen, *Anal. Methods*, 2018, **10**, 3402–3407.
33 Y. S. Kim, J. H. Kim, I. A. Kim, S. J. Lee, J. Jurng and M. B. Gu, *Biosens. Bioelectron.*, 2010, **26**, 1644–1649.
34 Y. Luo, J. Xu, Y. Li, H. Gao, J. Guo, F. Shen and C. Sun, *Food Control*, 2015, **54**, 7–15.
35 Y.-M. Sheng, J. Liang and J. Xie, *Molecules*, 2020, **25**, 2144.
36 R. Elghanian, J. J. Storhoff, R. C. Mucic, R. L. Letsinger and C. A. Mirkin, *Science*, 1997, **277**, 1078–1081.
37 S.-a. Supharoek, W. Siriangkhawut, K. Grudpan and K. Ponhong, *Molecules*, 2022, **27**, 3261.
38 Y. Sun, X. Yang, J. Hu, F. Ji, H. Chi, Y. Liu, K. Hu, F. Hao and X. Wen, *Talanta*, 2024, **274**, 126036.
39 I. C. Gonçalves, S. Soares and F. R. P. Rocha, *Microchem. J.*, 2023, **188**, 108461.
40 B. Jain, R. Jain, R. R. Jha, A. Bajaj and S. Sharma, *Green Anal. Chem.*, 2022, **3**, 100033.
41 D. Minh-Huy, L.-T. Anh-Dao, N. Thanh-Nho, L. Nhon-Duc and N. Cong-Hau, *Food Chem.*, 2023, **401**, 134147.
42 S. Soares and F. R. P. Rocha, *Microchem. J.*, 2021, **162**, 105862.
43 R. Urapen and P. Masawat, *Int. Dairy J.*, 2015, **44**, 1–5.
44 J. Song, X. Liu, X. Zhang, J. Fan, R. Zhang and X. Feng, *Talanta*, 2023, **265**, 124874.
45 P. Masawat, A. Harfield and A. Namwong, *Food Chem.*, 2015, **184**, 23–29.
46 S.-a. Supharoek, K. Ponhong, W. Siriangkhawut and K. Grudpan, *Microchem. J.*, 2019, **144**, 56–63.
47 B. Weerasuk, S.-a. Supharoek, K. Grudpan and K. Ponhong, *J. Iran. Chem. Soc.*, 2022, **19**, 741–751.
48 K. Kiwfo, S. Suteerapataranon, I. D. McKelvie, P. Meng Woi, S. D. Kolev, C. Saenjum, G. D. Christian and K. Grudpan, *Microchem. J.*, 2023, **193**, 109206.
49 K. Ponhong, W. Siriangkhawut, C. Y. Lee, N. Teshima, K. Grudpan and S.-a. Supharoek, *RSC Adv.*, 2022, **12**, 20110–20121.
50 E. C. B. A. Alegria, A. P. C. Ribeiro, M. Mendes, A. M. Ferraria, A. M. B. Do Rego and A. J. L. Pombeiro, *Nanomaterials*, 2018, **8**, 320.
51 P. He, L. Shen, R. Liu, Z. Luo and Z. Li, *Anal. Chem.*, 2011, **83**, 6988–6995.
52 J. Kim, K. Lee, C. T. Yavuz and Y. S. Nam, *Chem. Eng. J.*, 2024, **487**, 150529.
53 T. Ahmad, M. A. Bustam, M. Irfan, M. Moniruzzaman, H. M. A. Asghar and S. Bhattacharjee, *Biotechnol. Appl. Biochem.*, 2019, **66**, 698–708.
54 A. Sebastian, A. Nangia and M. N. V. Prasad, *J. Hazard. Mater.*, 2019, **371**, 261–272.
55 J. Zhang, F. Myasein, H. Wu and T. A. El-Shourbagy, *Microchem. J.*, 2013, **108**, 198–202.
56 B. Wang, T. Ezejias, H. Feng and H. Blaschek, *Chem. Eng. Sci.*, 2008, **63**, 2595–2600.
57 A. Gałuszka, Z. M. Migaszewski, P. Konieczka and J. Namieśnik, *TrAC, Trends Anal. Chem.*, 2012, **37**, 61–72.
58 F. Pena-Pereira, W. Wojnowski and M. Tobiszewski, *Anal. Chem.*, 2020, **92**, 10076–10082.